Sharp Cutoff Microwave Filters*

GEORGE OLTMAN†, SENIOR MEMBER, IRE

Summary—A class of sharp cutoff filters using combinations of lumped constant and distributed constant reactance have been analyzed and a test made of one type. The filters are developed in accordance with image parameter theory and are *m*-derived. Both high-pass and low-pass types are analyzed. The improvements over previous sharp-cutoff image parameter filters are predictable band limits and more predictable response. The derivations hold for all frequencies and are not approximations good only for short lengths of distributed constant reactance. Also, this class of filters have much sharper cutoffs than can be obtained with an equivalent number of sections designed using modern network theory.

Some of these filters have fairly flat response close to the sharp-cutoff and are useful as end-matching sections. Curves and design equations are presented for three types—two high-pass and one low-pass filter.

A seven-section high-pass filter was designed and tested. Its cutoff rate was 87db in a 3 per cent bandwidth located in the 300-Mc region. The pass-band width was greater than 30 per cent.

Introduction

A CLASS OF *m*-derived image-parameter filters and an experimental high-pass filter are described which make use of lumped and distributed constant filter elements. The prototype filter sections have been previously reported[1] but the *m*-derivations presented here have not. Pseudo *m*-derivations of distributed-constant filters have been used before,[2] but these were approximations to the exact image-parameter theory. The work presented here follows the exact image-parameter theory, and has the advantage that the image impedance is unaffected by the *m*-deriving process and that the exact cutoff frequency can be calculated.

M-derivation has two features which are useful in filter design. First, the *m*-derived sections can be used to match the filter, which generally has a variable transfer impedance, to a constant impedance load or generator. Second, *m*-derivation of the prototype sections introduces resonances having high attenuation which allow the creation of extremely sharp-cutoff high-pass or low-pass filters. To obtain such sharp cutoffs using modern network theory is difficult and impractical. The high attenuation resonances are positioned at the edge of the stopband to form the sharp cutoff. The resonant frequencies are determined by the values of *m* in each section. Similarly, resonances can be placed throughout the remainder of the stopband to achieve over-all high insertion loss. Because the pass band image impedance is independent of the *m* values, the pass band is unaffected.

The filters described here use low-loss distributed-constant elements combined with lumped-constant coupling elements arranged for minimum volume. The total volume is essentially the same as similar filters designed using modern network theory, but not having as sharp a cutoff. Further, the image-parameter design allows changes in the number of sections without complete redesign.

Derivation

The *m*-derived filters are derived[3,4] from the prototype filter sections shown in Fig. 1. C and L are lumped reactances and Z_L is a distributed constant reactance. Z_L is the characteristic impedance of the shunt transmission lines. There are three possible configurations which differ in reactance elements and termination of the shunt line. The two basic sections are those shown in Fig. 1. The third is a variation of the high-pass filter using an open-circuited line. It is not possible to have a short-circuited version of the low-pass filter because the filter would be shorted at low frequencies by the stub.

The image impedances of the filter sections are most easily derived using matrix algebra.[5] The derivation is not repeated here. However, the image impedance equation for each filter section is given on the graph of its frequency characteristics. All of the parameters have been normalized to simplify the equations and are tabulated on each graph. The normalized frequency variable is $r=\omega/\omega_L$. It is the ratio of operating frequency ω to the frequency ω_L at which the line Z_L would be one-half wavelength long. ν and ρ are used to describe the high-pass equations shown in Figs. 2 and 3. σ and η are used to describe the low-pass equation shown in Fig. 4.

M-Derived Filter Sections

An *m*-derived T filter section has the same characteristic image impedance as its prototype T section. That is, the image impedance is independent of the parameter *m*. However, the image impedance of the π equivalent of the *m*-derived T section is not independent of *m*. Thus, if a half-section *m*-derived filter is fabricated, the image impedance looking into one side will be

* Received June 27, 1962; revised manuscript received, September 24, 1962. This investigation was performed while the author was with the RANTEC Corporation. The work was sponsored by the Wright Air Development Division on Contract No. AF 33(616)-6735, Task No. 43091.

† Space Technology Laboratories, Inc., Redondo Beach, Calif. Formerly with RANTEC Corporation, Calabasas, Calif.

[1] Harvard Univ. Radio Res. Lab., "Very High Frequency Techniques," McGraw-Hill Book Co., Inc., New York, N. Y., vol. 2, pp. 705 and 710; 1947.

[2] *Ibid.*, see also p. 708.

[3] J. J. Karakash, "Transmission Lines and Filter Networks," The Macmillan Co., New York, N. Y., p. 278; 1950.

[4] O. Zobel, "Theory and design of uniform and composite electric wave filters," *Bell Sys. Tech. J.*, vol. 2, pp. 11–46; January, 1923.

[5] D. V. Geppert, "Image Impedance Design of TEM, Mode Microwave Filters," Electronic Defense Laboratory, Mountain View Calif., Rept. No. ED1-E6; 1955.

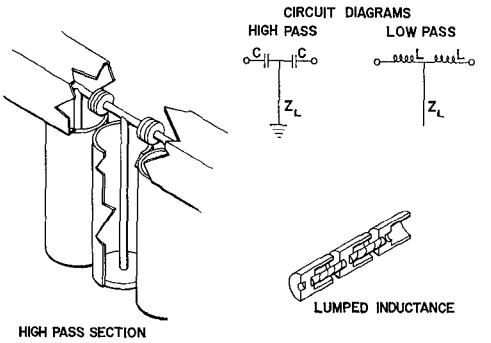

Fig. 1—Prototype filter sections.

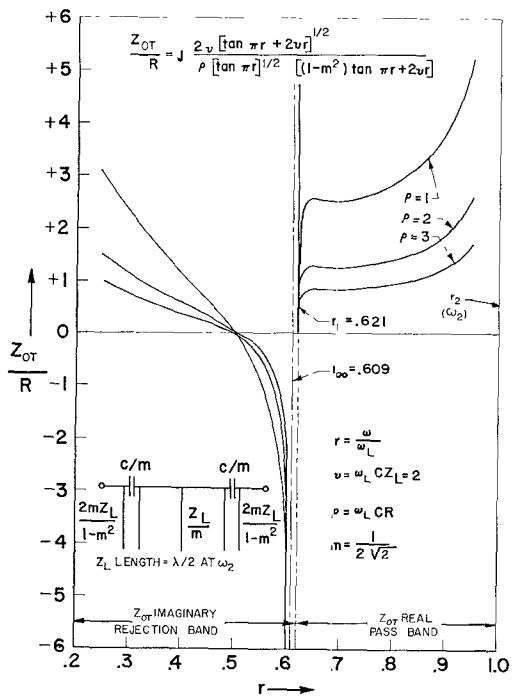

Fig. 2—T equivalent of m-derived π section.

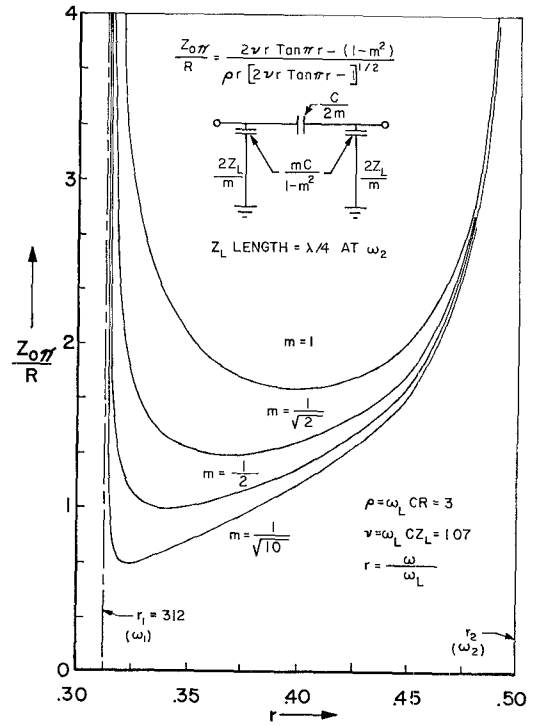

Fig. 3—π equivalent of m-derived T.

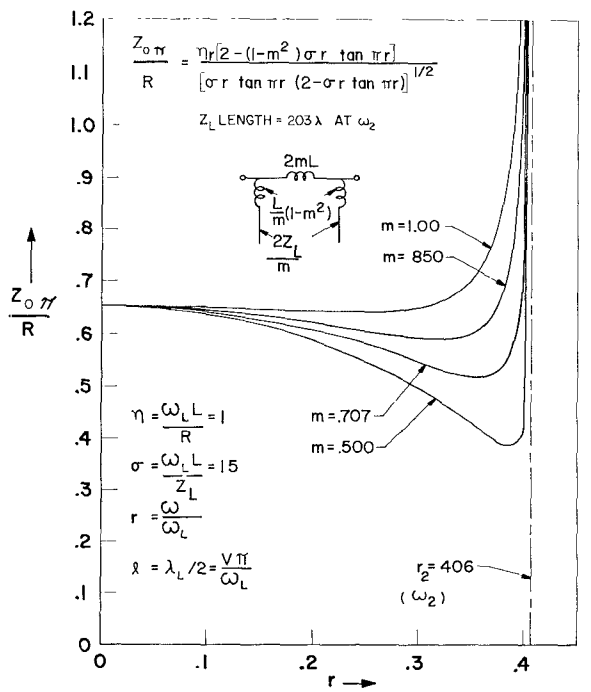

Fig. 4—π equivalent of an m-derived T section.

dependent on m and looking into the other side will be independent of m. This quality is useful in matching the generator or load to the center sections of a filter.

For the sharp cutoff filters, however, the frequencies of infinite attenuation which are determined by m are most important. These attenuation peaks are a consequence of the introduction of an additional reactance element by the derivation process which creates new or modified resonances. The new elements may be in either the series or shunt arms. Series arm elements form parallel resonances with the existing elements and shunt arm elements form series resonances with the existing element. Series arm elements create new resonances, and shunt arm elements modify existing resonances.

The frequencies of infinite attenuation are designated by r_∞ on the graphs. Other infinite attenuation frequencies may exist, but they are not a function of m. These are determined by other zero or infinite image impedances found on the graphs. Of course, it is not possible to achieve the discussed infinite attenuations. These are theoretical lossless attenuations. Any loss in the section will reduce the maximum attenuation.

Sharp Cutoff Filter Design

The sharp cutoff filter has two end-matching sections plus the required number of center sections to achieve the required stopband performance.

The end-matching half-sections of the filter may be chosen from any of the sections which have the desired (near) constant image impedance over the desired passband. This half-section will then match the load (or generator) to the center sections of the filter. M-derived center sections can then be arbitrarily used to position frequencies of infinite attenuation as required throughout the stopband. The interior section pass-band image impedances will all be independent of m yielding a completed filter having the image impedance of the end-matching half-sections.

The number of sections and frequencies of infinite attenuation depends on the desired sharpness of cutoff and minimum insertion loss. The optimum placement of the high attenuation peaks cannot easily be predicted. Circuit losses will strongly affect the peak attenuation. Also, nearness to cutoff will lower attenuation peaks. Attenuation measurements using one section and varying the positions of the peaks will ordinarily yield enough information to place the attenuation peaks.

Cutoff Frequency and Frequencies of Infinite Attenuation

A. High-Pass Filters[6]

The upper cutoff frequency for the high-pass filters is determined by the length of the line Z_L. This line is one-quarter wavelength for shorted stubs and one-half wavelength for open-circuited stubs. The lower cutoff frequency is determined by the terms of the image impedance equations yielding poles or zeros and having the general forms

$$[\tan \pi r + 2\nu r]$$

or

$$[2\ \nu r \tan \pi r - 1].$$

These terms are taken from the impedance equation in Figs. 2 and 3. Setting the terms separately equal to zero yields the cutoff frequencies as a function of the parameter ν. The solution is plotted in Fig. 5 for both the open and shorted high-pass filter types.

B. Low-Pass Filters

The upper cutoff frequency of the low-pass filters is determined by setting equal to zero the term

$$[2 - \sigma r \tan \pi r],$$

which is taken from Fig. 4. The solution is not plotted.

C. Frequencies of Infinite Attenuation

The frequencies of infinite attenuation are determined by the zeros or poles of the image impedance equation in the stopband. The high attenuation frequency which is a function of m is determined by a zero value of the bracketed term of the type

$$[(1 - m^2) \tan \pi r + \nu r].$$

The solution can be determined from Fig. 6. It yields a value of ν_∞ which can be used in place of ν in Fig. 5. Fig. 5 then yields the ratio of the frequency of infinite attenuation ot ω_L rather than the ratio of the lower cutoff frequency to ω_L for high-pass filters.

Image Impedance Curves

Figs. 2, 3 and 4 are graphs of image impedance vs the normalized frequency variable r. These filter sections represent the best of the m-derived types having fairly flat responses near cutoff, and hence, are suited for end-matching half-sections. Only one low-pass filter is presented (Fig. 4), but its response is excellent. The high-pass filter with Z_L shorted, (Fig. 3) will have one-half the length of the open-circuited high-pass filter, (Fig. 2). It is difficult to compare the bandwidth of the two. For approximately the same response, the shorted filter requires $Z_L = 1.33\ R$ and the open filter requires $Z_L = 2.8\ R$. The former is easiest to fabricate when $R = 50$ ohms. For the high-pass filters, the upper cutoff frequency ω_2 is determined by the first resonance of the line Z_L. Thus, $\omega_2 = \omega_L(r_2 = 1)$ for the open stub filter and $\omega_2 = \frac{1}{2}\omega_L(r_2 = 0.5)$ for the shorted stub filter. Lower cutoff is ω_1 or r_1. For the low-pass filter, lower cutoff is at zero frequency.

The image impedances $Z_{0\pi}$ and Z_{0T} are normalized by

[6] The high-pass filters are not truly high-pass in the normal sense of the term. What is meant is that the high-pass filters have their flat response on the high side of the lower cutoff.

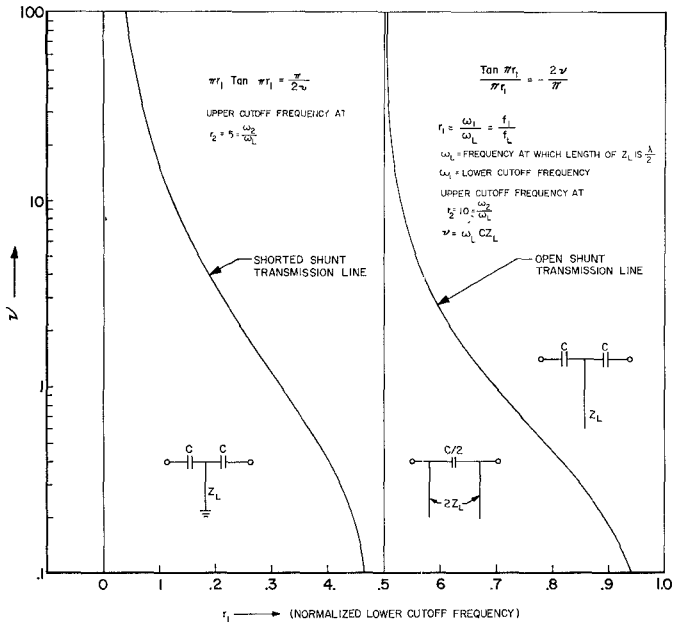

Fig. 5—Design curve—cutoff frequency for high-pass filters.

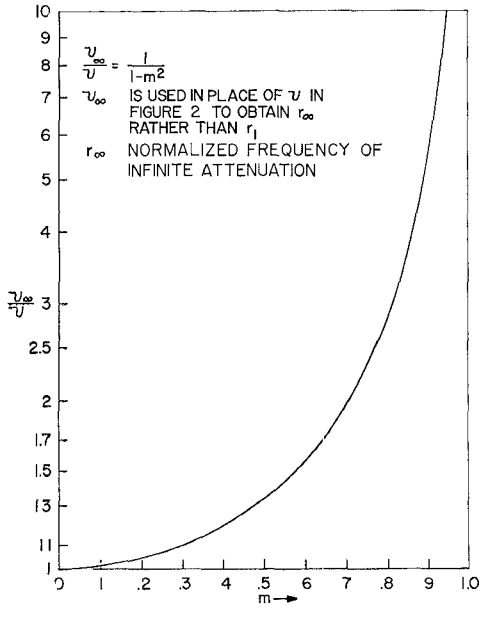

Fig. 6—Design curve—frequencies of infinite attenuation.

the terminal resistance R. The circuit constants C, L, Z, and R are interrelated and normalized by the parameters ν, ρ and σ (defined on appropriate graphs). ω_L is used in computing the reactances which define these parameters. ρ and η are used to set the impedance level at which the filter operates.

The circuit diagrams on each graph show the new values (different than the prototype) of inductance, capacitance, and line impedance for each of the analyzed filters.

Fabrication

The experimental filters were high-pass and were constructed using shunt coaxial lines and series capacitors. Fig. 1 shows the general type. Fig. 7 shows an experimental model using stripline circuitry combind with shorted coaxial stubs. The photograph shows only two of the possible seven stubs being used. The experimental version tested and described below, however, utilized open-circuited stubs rather than the short-circuited stubs shown in Figs. 1 and 7. Fig. 8 shows a complete 7-section filter and Fig. 9 shows some of the internal construction. The capacitors were mating coaxial rods and cylinders insulated with thin Teflon adhesive tape. The m-derived sections also required capacitors in series with the stubs. These were similarly fabricated and located at the T junction in Fig. 1.

All stubs were measured and cut to half a wavelength at upper cutoff frequency and assembled. Using a capacitance bridge, the capacitors were adjusted to the theoretical values. The capacitors were then trimmed while observing the pass-band VSWR.

Experimental Results

The experimental filters were built for the lower UHF band. The specification required that the attenuation below lower cutoff increase to 80 db in approximately 3 per cent bandwidth. The specification was achieved using seven sections. The pass band width was approximately 30 per cent.

The number of sections required to meet the specification was arrived at after measuring the stopband attenuation of a single m-derived section. This section was constructed using the exact materials, conductor sizes and finishes of the final filter so it would be representative of the resonator Q. By moving its frequency of infinite attenuation about within the stopband and observing the response, the required number of m-derived sections could be closely estimated. Such a technique presents no redesign difficulty for, if the estimate is wrong, a section can be inserted or removed without affecting the remaining sections.

Five of the seven sections were m-derived having the frequencies of infinite attenuation adjusted to 0.961, 0.957, 0.957, 0.950 and 0.870 of the lower cutoff frequency. The end-matching half-sections were not m-derived because adequate match to the generator was achieved without it. These sections also had frequencies of infinite attenuation, but were not functions of the parameter m.

Fig. 10 shows the insertion loss and VSWR. The stopband insertion loss rises to 87 db in 3 per cent bandwidth. Four of the m-values were utilized to create the sharp cutoff and are closely bunched just below cutoff. The fifth was adjusted to improve the rejection in the center of the stopband. The selected frequencies were not optimum, but were the first guesses at the proper frequencies. Only a slight readjustment would be necessary to eliminate the two insertion loss excursions below the specification limit.

The pass band insertion loss is below 1.6 db through-

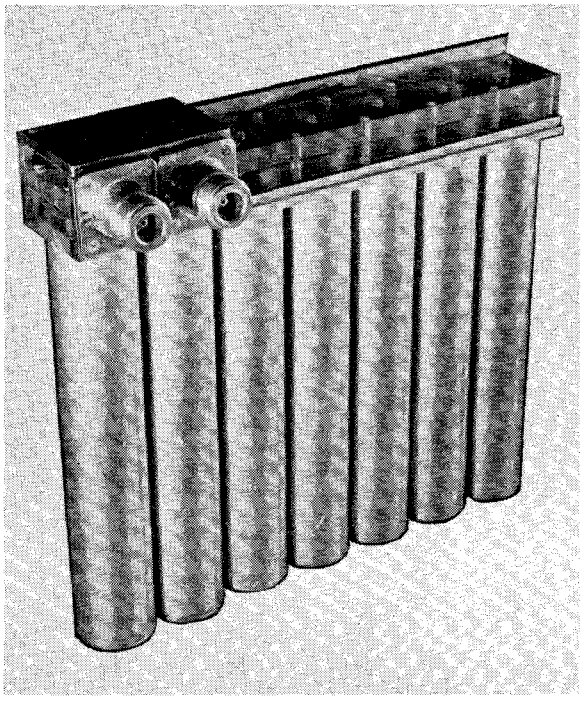

Fig. 7—Stripline—coaxial hybrid filter.

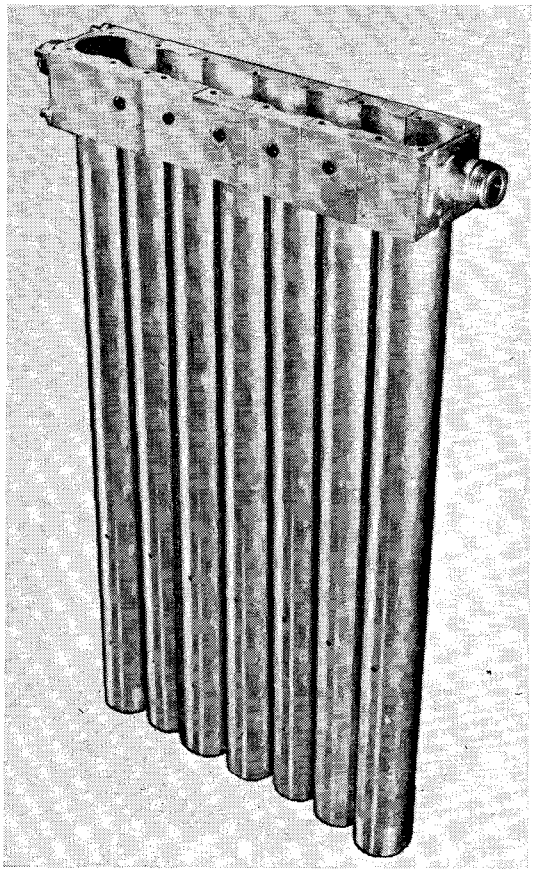

Fig. 8—Seven section coaxial filter.

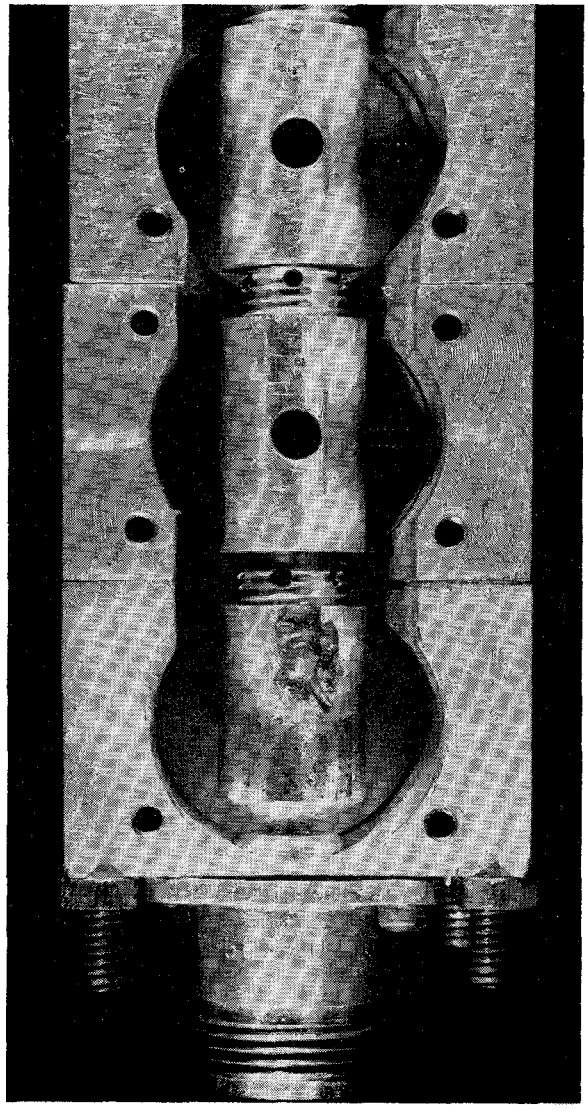

Fig. 9—Internal construction of coaxial filter.

out the band. Hopefully this could be reduced with more care in fabrication by trimming the filter using a swept frequency generator and display.

Fig. 11 shows the measured impedance of a more carefully constructed three-section filter. The pass band response very rapidly approached the Smith Chart center and then continued very slowly circling the center yielding a broad low VSWR pass band.

The two end sections are end-matching half-sections exactly like those of the seven-section filter. The center section is an m-derived section having its frequency of infinite attenuation at 0.98 that of lower cutoff. Fig. 12 shows the insertion loss of the filter. Note that the peak attenuation at 303 Mc is greatly reduced because of the nearness to cutoff.

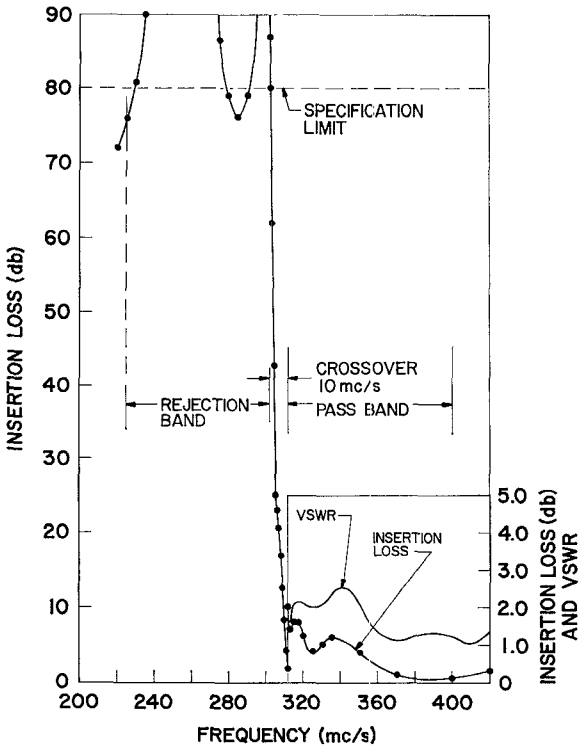

Fig. 10—Seven section coaxial filter.

Conclusions

Using the technique of m-deriving, a class of microwave filters has been created which yield very sharp cutoffs. The particular embodiment chosen allows fabrication of these filters in a space equal to that of more common coupled-resonator filters having much less sharp cutoffs. The theoretical design curves allow reasonably accurate design of practical filters with very little trimming.

The technique of m-deriving has not been previously applied to distributed-constant microwave filters, although, as mentioned, pseudo m-derived filters have been reported.[2] There are other filter types which can be investigated which may lead to even more useful filters. Noteworthy are m-derived filters using distributed inductances and capacitances entirely rather than combining distributed and lumped reactance as done here. Such filters should extend the usefulness of this type to substantially shorter wavelengths.

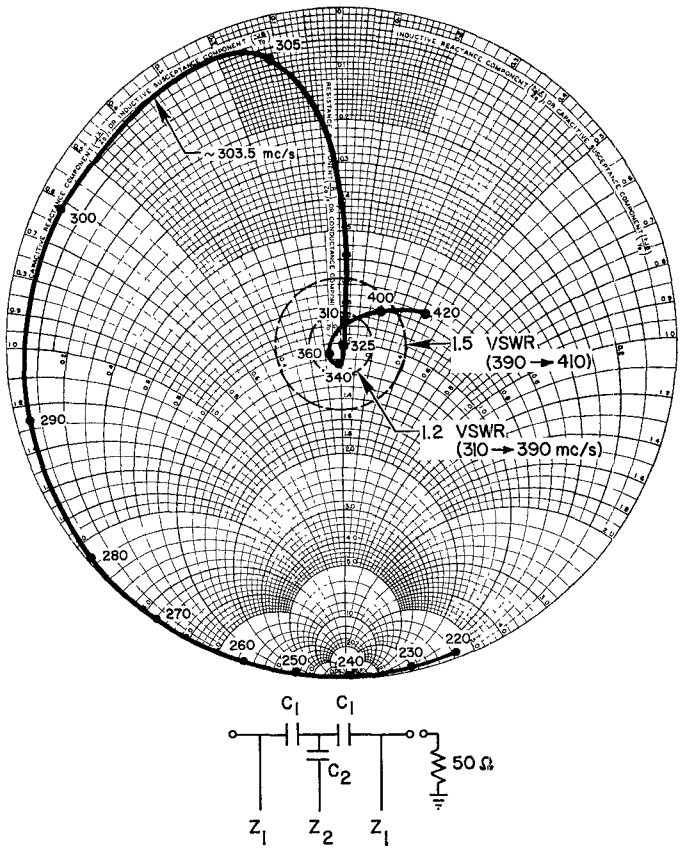

Fig. 11—Three section filter.

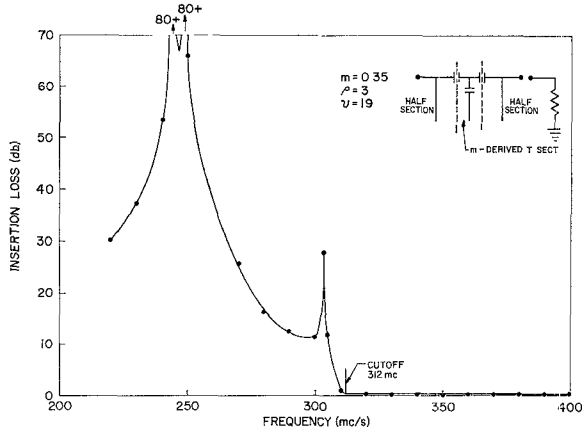

Fig. 12—Three section filter.